IJPSR (2020), Volume 11, Issue 12 **(Research Article)**

INTERNATIONAL JOURNAL OF PHARMACEUTICAL SCIENCES AND RESEARCH

Received on 18 February 2019; received in revised form, 28 March 2019; accepted, 17 April 2019; published 01 July 2019

EFFECT OF TEMPERATURES ON STRUCTURAL, MORPHOLOGICAL AND BIO-PROPERTIES OF ZINC FERRITE NANOPARTICLES

B. Jyothish and John Jacob *

Department of Physics, University of Kerala, Mar Ivanios College, Thiruvananthapuram - 695015, Kerala, India.

Keywords:

Ferrites, Nanoparticles, Annealing, Capping agents, Co precipitation method

Correspondence to Author:
Dr. John Jacob

Assistant Professor,
Department of Physics,
Mar Ivanios College, Nalanchira,
Thiruvananthapuram - 695015,
Kerala, India.

E-mail: john.jacob@mic.ac.in

ABSTRACT: Zinc Ferrite nanoparticles were prepared by chemical co-precipitation method, using PEG as the capping agent. The synthesized materials were annealed at different temperatures such as 400, 500, 600, 700 and 800 °C and the structural characterization studies were conducted by X-Ray Diffraction (XRD), Fourier Transform Infrared Spectrometer (FTIR), UV-Visible Spectroscopy and Field Emission Scanning Electron Microscopy (FESEM). On heat treatment of the as prepared samples, crystallite size was observed to increase from 5 nm-22 nm. XRD pattern confirmed the single crystalline phase of developed particles. It was observed that the particle size and X-ray density of the annealed $ZnFe_2O_4$ nanoparticles linearly increased with increase in annealing temperature and decrease in lattice parameters. The calculated micro strain values were found to be decreasing with increasing annealing temperatures. The nanoparticle size was confirmed using SEM measurements. Furthermore FTIR mapping confirmed the presence of $ZnFe^2O^4$ nanoparticles. The calculated band gap (Eg) of zinc ferrite nanoparticles decreases with increase in temperature. The antibacterial activity of $ZnFe^2O^4$ nanoparticles was studied against gram negative E-coli pathogenic bacteria. DPPH assay was used to determine the antioxidant activity of the compound. *In-vitro* anticancer activity was screened by MTT assay against MCF-7 (Human breast adenocarcinoma) cell and A549 (Lung Cancer) cell line. It was observed that the increase in particle size and annealing temperature influence the inhibition rate of these bio properties. The investigation points out that $ZnFe_2O_4$ nanoparticle possess less viability with increase in concentration towards MCF-7 cell than A549 cell.

INTRODUCTION: Ferrites have a major role in scientific and technological areas, because of its wide range applications such as magnetic resonance imaging, magnetic recording, catalyst, high-frequency coils and radar absorbing materials while comparing with pure metals, Ferrites are superior magnetic materials due to their high resistivity, magnetic properties, fair cost *etc.*

QUICK RESPONSE CODE

DOI: 10.13040/IJPSR.0975-8232.11(12).6391-01

The article can be accessed online on www.ijpsr.com

DOI link: http://dx.doi.org/10.13040/IJPSR.0975-8232.11(12).6391-01

Zinc ferrite ($ZnFe_2O_4$) nanoparticles exhibit excellent magnetic permeability, low eddy current, non-toxicity, high stability *etc.* [1, 2] Zinc Ferrite nanoparticles can be prepared by various methods including hydrothermal, sol-gel, electrochemical, co precipitation method, high energy ball milling *etc.* [3, 4]

Among various methods, co precipitation technique was the efficient method because of its control over the surface morphology, simplicity of the procedure, low reaction temperature and eco-friendliness [5]. Zinc ferrite normally exhibits spinel structure. It can be represented as $[A][B]2O_4$ where A and B are the cations Zn^{2+} and Fe^{3+} in tetrahedral and octahedral sites of the FCC structure,

respectively [6, 7]. The prepared samples were subjected to 5 different calcination temperature such as 400, 500, 600, 700 and 800 °C for 4 h. The characterization of the synthesized nano particles were carried out by P- XRD, UV-Visible Spectroscopy, FESEM and FTIR [8, 9]. In addition to the characterization studies, the antibacterial, anti-fungal, antioxidant activity and *in-vitro* anticancer activity against MCF -7 (Human breast cancer, adenocarcinoma) and A549 (Lung cancer) of the synthesized $ZnFe_2O_4$ nano-particles were analyzed. It is widely applied for Bio-medical applications because of the ease of implementation and less hazardous materials [10, 11].

Experimental Section:

Preparation of Zinc Ferrite Nano-particles: $ZnFe_2O_4$ nano particles were synthesized by co precipitation method by using ferric nitrate ($Fe(NO_3)9H_2O$), zinc nitrate ($Zn(NO_3)2$) and ammonium carbonate $(NH_4)2CO_3$ as reagents, PEG as the capping agent and NaOH as the precipitating agent to precipitate the required sample.10.1 g of 0.5M$Fe(NO_3)2$, 7.43 g of 0.5 M ($Zn(NO_3)2$) were accurately weighed and dissolved in 100 mL distilled water. The evenly mixed solution was filled in a burette. The weighed of 20 g of 0.1 MPEG, 1 g of 0.5M NaOH and 3.92 g of 0.5M $(NH_4)2CO_3$ were taken and were uniformly dissolved in 150 mL distilled water. The solution was poured into a conical flask and was subjected to magnetic stirring by adding the solution taken in burette drop by drop. Magnetic stirring was continued till the whole solution in burette was added to the mixture. The formed brown coloured precipitate was filtered out after centrifugation (4000 rpm) for 15 min. The precipitate was washed several times with distilled water. The separated precipitate was heated to 70-80 °C for drying and after that the precipitate was grinded. The prepared samples were annealed at different temperatures.

***In-vitro* Anti-cancer Effect Determination by MTT Assay:** MCF – 7 (Human breast adenocarcinoma) cell was collected from NCCS (National Center for Cell Sciences), Pune, India. The viability of cancer cells were measured by direct observation of cells inverted phase contrast microscope and adopted by MTT assay, which can be used to identify the viability of nano-particle treated cells [12, 13].

The cell line was cultured in 25 cm^2 tissue culture flask with Dulbecco's modified Eagle medium accumulated with 10% of PBS, sodium bicarbonate L-glutamine. The antibiotic solution containing amphotericin B (2.5 µg/mL), penicillin (100 µg/mL) and streptomycin (100 µg/mL). The cultured cell lines were kept at 37 ºC in a humidified 5% carbondioxide incubator. 1mg of sample was weighed and dissolved in 1 mL Dulbecco's modified, Eagle medium using a cyclomixer. The sample solution was filtered through 0.22 µm syringe filter to ensure the sterility.

Anticancer Evaluation: The growth medium was removed after 24 h and freshly prepared each compound in 5% Dulbecco's modified Eagle medium was 5 times continuously diluted by two fold dilution (100 µg, 50 µg, 25 µg, 12.5 µg, 6.25 µg in 500 µL of 0.05 DMEM) and each concentration of 100 mL was mixed in triplicates at 37 °C in a humidified 5% carbon dioxide incubator. Non treated control cells were also maintained.

Anticancer Assay by MTT Method: 15 mg of MTT (sigma – M 5655) was reassembled in 3 mL PBS until dissolved and sterilized by filter sterilization. The sample content in wells was removed after 24 h of inhibition period and 30 µL of the reconstituted MTT solution was added to all test solution and cell control wells, the plate was shaken well, after that the sample was incubated at 37 ºC in a humidified 5% CO_2 incubator for 4 h. The supernatant was ignored after the incubation period and 100 µL of MTT solubilization solution was mixed and the wells were mixed gently by pipetting up and down in order to solubilize the formazan crystals. Micro plate reader at a wave length of 540 nm was used to measure the values of absorbance. The percentage of growth inhibition was calculated using equation 1.

Percentage of viability = (Mean Optical Density of Samples) / (Mean Optical Density of Control group) × 100 ---------- (1)

Antioxidant Activity (Evaluation of DPPH Free radical Scavenging Activity): Antioxidant are substance which can protect our cells against the effect of free radicals which causing heart diseases, cancer and other diseases [14]. Hence, it is necessary to design certain materials, which possess anti-oxidant capability [15].

DPPH assay can be used to determine the radical scavenging activity of the compounds. Here ascorbic acid at 10 mg/mL and DMSO were used as the reference material. After the addition of sample the solution was analyzed at 517 nm which was compared with the reference material. 11-diphenyl -2-picryl hydroxyl (DPPH) which appeared as pink colour when existed as a free radical and when get scavenged (DPPH-H) its colour changes to yellow. When the anti-oxidant was introduced the following reaction will occur,

$$DPPH+[H-A] \rightarrow DPPH - H + (A) \text{ ---------- (2)}$$

Pink Yellow

Where DPPH gets reduced to DPPH-H thereby the absorbance decreases. The variation in decoloration shows the scavenging potential of antioxidant present in the sample.

0.1 mM free radical solution is prepared by dissolving 4 mg of DPPH in 100 mL ethanol. Stock solution (10 mg/mL) of the sample was prepared and from this different volume such as 1.25 µg/mL-20 µg/mL (12 µg/mL-200 µg/mL) were made up to final volume of 20 µL with DMSO and to this 1.48 mL of DPPH (0.1 mM) solution were added. Control was prepared by adding an equal amount of distilled water as that of sample. The solutions were incubated in dark conditions at room temperatures for 20 min and absorbance was measured at 517 nm. The % inhibition is calculated by equation (3).

$$\% \text{ inhibition} = (\text{Control} - \text{test}) / \text{Control} \times 100 \text{ ---------- (3)}$$

Antifungal Activity (Agar Well Diffusion Method): Antifungal activity of $ZnFe_2O_4$ samples were analyzed using Agar well diffusion method, in which *Aspergillus niger* (ATCC 16404) was used as the culture of test organism. This activity was based on the principle that when samples were introduced into the medium, the antifungals present in the sample interact with the test organisms, which were seeded in a plate. The whole process was carried out on petriplates of 100 mm, which were coated with Potato dextrose agar medium prepared by dissolving 39 g of potato dextrose agar medium in 1000 mL distilled water. After that the dissolved medium was autoclaved at 15 lbs pressure at 121 ºC for 15 min.

This will be poured over the petriplates and overnight grown species of *Asperigillus niger* was swabbed. Samples heated at different temperature were added to the well of 10mm bored using a well cutter at different concentrations say 250, 500 and 100 µg/mL. The zone of inhibition was analyzed by comparing with the standard clotrimazole at a concentration of 10 mg/mL after incubating over-night at room temperature. The resulting zone will be uniformly circular as there will be confluent lawn of growth, and the diameter of zone was measured in millimeter.

Antibacterial Activity (Agar-Well Diffusion Method): The antibacterial activity of zinc ferrite nanoparticles samples was studied against *Escherichia coli* (ATCC 25922) by using Agar-well diffusion method [16]. The experiment was carried out on 100 mm petriplates coated with Muller Hinton Agar medium prepared by dissolving 33.8 g of MHI Agar media in 1000 mL distilled water. Dissolved medium was autoclaved at 15 lbs. pressure at 121 ºC for 15 min. The auto-claved medium was mixed well and poured on to 100 mm petriplates (25-30 mL/plate) while still molten. Nutrient broth was prepared by dissolving 13 g of commercially available nutrient medium in 1000 mL distilled water and boiled to dissolve completely. This medium was dispensed and sterilized by autoclaving at 15 lbs pressure (121 ºC) for 15 min. Streptomycin was used as the anti-bacterial agent at a concentration of 10 mg/mL

Petriplates coated with 20 mL Muller Hinton Agar medium seeded with bacterial culture of *E. coli*, was growth of culture adjusted according to McFarland standard 0.5%. The antibacterial activity of sample was analyzed by adding different concentration such as 250, 500 and 1000 µg/mL on the wells of approximates 10 mm which was bored using a well cutter. Plates were incubated at 37 ºC for 24 h. Antibacterial activity was measured from the diameter of inhibition zone formed around the well. The resulting zone of inhibition will be uniformly circular as there will be a confluent lawn of growth [17].

RESULTS AND DISCUSSION:

XRD Studies: The XRD patterns of the annealed $ZnFe_2O_4$ nano-particles were recorded using a Philips x1 pert pro diffractometer with Cu-kα, (λ =

1.54056 Å) radiation in the range of 20 ~10 - 70º. The source was operating under an accelerating voltage of 40 kV with a tube current of 30 mA.

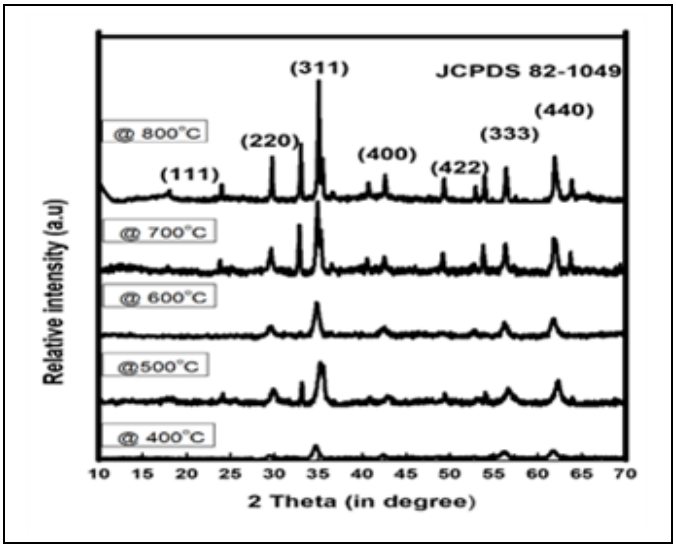

FIG. 1: XRD PATTERNS OF $ZnFe_2O_4$ NANOPARTICLES ANNEALED AT DIFFERENT TEMPERATURES

Crystallite size of the sample at different annealing temperature were calculated using Debye Scherer formula for peaks corresponding to (311) plane,

$$D = B\lambda / (\beta \cos\theta) \text{ - - - - (4)}$$

Where D is the crystallite size, λ is the wavelength of Cu - k∝, β is the full width of half maximum of the diffraction peaks and θ is the Bragg's angle. It could be shown from the **Table 1** that as the calcination temperature increases there is an increase in the crystallite size (D) from 5 to 22 nm.

This is because at high temperature diffusion of grains becomes more rapid which causes better organization of the sample. The XRD profile indicates the formation of single phase FCC spinal structure. In the sample the peak intensity was very sharp and narrow in nature which confirmed that the samples were at high quality, fine grain size and with good crystallinity [18]. The lattice constant a is measured by using Bragg's equation, for prominent (311) Peak

$$A = d\_hkl \sqrt{(h^2+k^2+l^2)} \text{---------- (5)}$$

The specific surface area (s) can be calculated by the relation,

$$S = 6/(d\_x*t)\text{----------(6)}$$

TABLE 1: CRYSTALLITE SIZE (NM), PARTICLE SIZE (NM), LATTICE CONSTANT A (Å), X-RAY DENSITY (DX), VOLUME (V), SPECIFIC SURFACE AREA (S), MICRO STRAIN (ε)

Temp (°C)	Crystallite Size (nm) XRD (Å)	Particle size (nm) SEM	Lattice Constant (a)	X-ray Density ρXRD (g/cm^3)	Volume (Å) 3(S) (m^2/g)	Specific Surface Area	Micro strain (Ɛ)
400 ºC	5	3.48	8.53202	5.15636	21.092	23.27	0.0065
500 ºC	5.98	4.49	8.44134	5.3242	601.498	18.845	0.0056
600 ºC	6.604	5.05	8.41584	5.737	596.063	16.91	0.0050
700 ºC	10.38	9.58	8.38154	5.439	588.805	10.63	0.0039
800 ºC	21.92	11	8.3523	5.496	582.644	4.9	0.0014

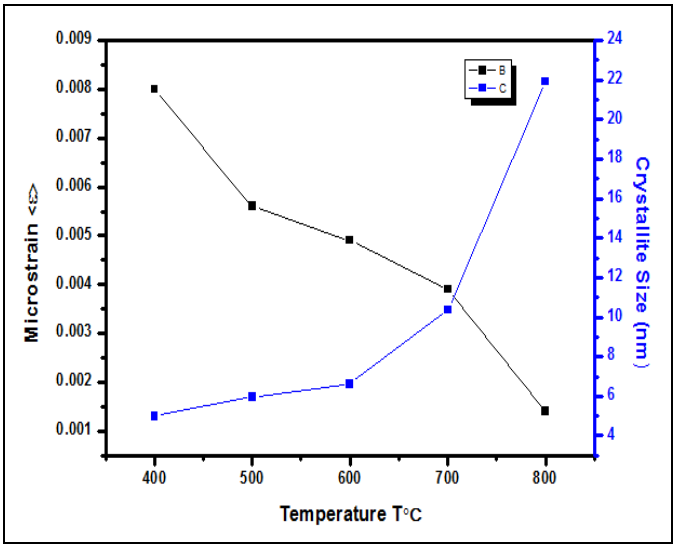

FIG. 2: VARIATION OF CRYSTALLITE SIZE AND MICRO STRAIN WITH CALCINATION TEMPERATURE

From the **Table 1** it was understood that the crystalline size and x-ray density (dx) were increased by increasing annealing temperature from 400 to 800 ºC, but the values of lattice parameter (a) decreases by increasing calcination temperatures. From the **Fig. 1** it was observed that an additional peak at 2θ=33.15° which represents the formation of secondary phase. The calculated value of lattice parameter for $ZnFe_2O_4$ was in good agreement with standard data 8.440Å from JCPDS card number 82-1049. It was observed that from the lattice parameters of the crystalline sample X-ray density (ρx) and bond lengths (A-O and B-O) and ionic radii (rA and rB) on A-site and B-site of all the samples can be measured by the following equations 6.

ρ_(x= (8 M)/〖Na〗^3)----------(7)

Where N is the Avogadro number and M is the molecular weight and

A-O = (μ-1/4)a√3) ----------(8)

B-O = (5/8-μ)a----------(9)

r_A = (μ-1/4)a√3-R_0---------- (10)

r_B = (5/8-μ)a-R_0---------- (11)

Where μ is the oxygen ion parameter (0.381Å) and Ro is the radius of oxygen ion (1.32Å)

To find the crystalline size and micro strain simultaneously in the sample William-Hall (W—H) equation is used [6].

β_hkl cos⁡θ_hkl=kλ/D+4εsin⁡θ_hkl------- (12)

Where D is the average crystallite size from W-H plot and micro strain can be represented as Ɛ. Micro strain is the measurement of the concentration of defects in the sample [19].

TABLE 2: THE VALUES OF BOND LENGTH (Å), IONIC RADII (Å)

Temp (°C)	Bond length (Å)		Ionic radii (Å)	
	A-O site	B-O site	rArB	
400 ºC	1.936	1.911	0.617	0.762
500 ºC	1.915	1.891	0.596	0.739
600 ºC	1.9096	1.855	0.590	0.733
700 ºC	1.902	1.877	0.583	0.725
800 ºC	1.895	1.870	0.576	0.718

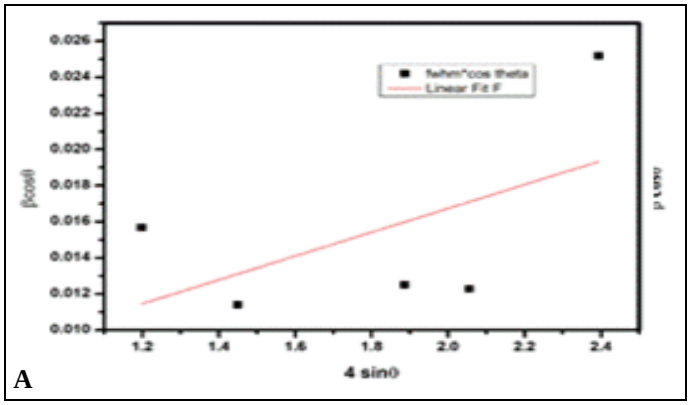

FIG. 3: WILLIAM-HALL PLOTS FOR ZINC FERRITE ANNEALED AT (A) 400, (B) 500, (C) 600, (D)700 AND (E) 800 °C

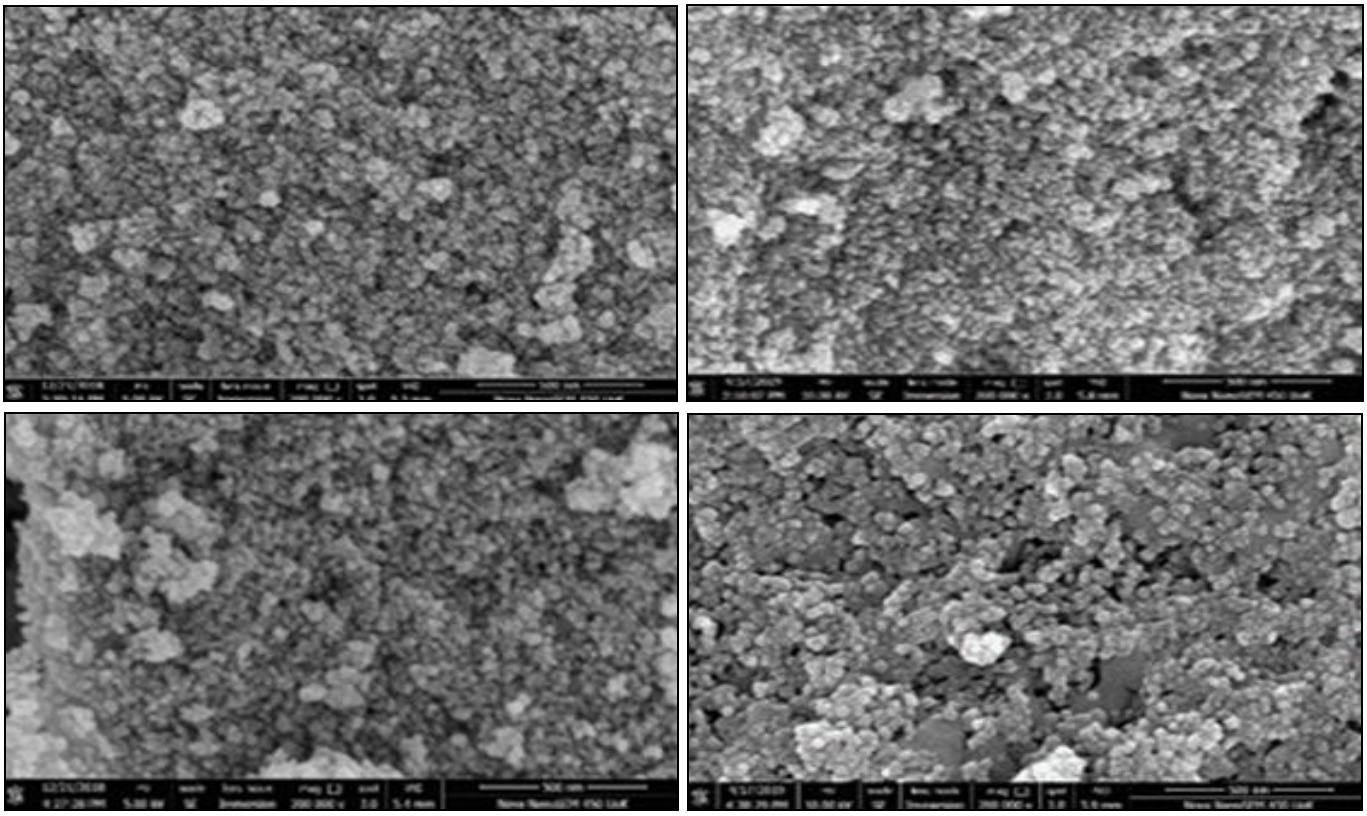

FIG. 4: FE-SEM IMAGES OF ZINC FERRITE NANOPARTICLES AT DIFFERENT ANNEALING TEMPERATURES

FE-SEM images at different magnifications of $ZnFe_2O_4$ nanoparticles were shown in **Fig. 4**. The figures revealed the spherical morphology of the particles. Particle sizes were nearly comparable with XRD crystallite sizes in **Table 1**. The formation small size particles resulted in extensive agglomeration ascribed to high surface energy.

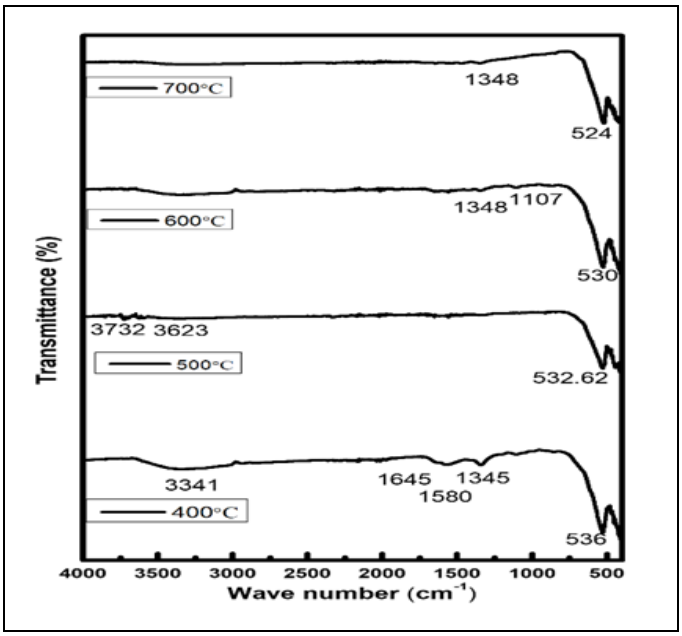

FIG. 5: FTIR SPECTRUM OF ZINC FERRITE NANO-PARTICLES ANNEALED AT DIFFERENT TEMPE-RATURES

FTIR Mapping: In order to confirm the spinal structured ferrites, FTIR studies were conducted at various temperatures. All the samples exhibited a peak near 550 cm^{-1} which indicates the Fe – Ostretching vibration, and the values found to be shift to lower frequency as temperature increases. Another absorption band was observed within the range of 380–450 cm^{-1} which corresponds with the Zn – Ostretching modes. These observations concluded that they were the characteristic peaks of $ZnFe_2O_4$ nano particles. FTIR analysis also helps to understand the nature of residual carbon in the sample. In the present study as the sample temperature increased the number of absorption band found to be decreasing.

Peak observed at 3343, 1645 and 1580 cm^{-1} at 400 ºC corresponds to OH, C=C and C=O stretching, respectively which disappeared as the temperature of the sample increased, but O-H bending vibration band near the range 1347 cm^{-1} was found to be present in the sample even at high temperature at almost same frequency. The disappearance of the peaks of residential carbon in sample was burned away during the annealing process.

Optical Analysis: The optical characteristics of $ZnFe_2O_4$ nanoparticles was studied by UV-Visible

absorption spectrum 20. The Tauc plot band gap Eg values of $ZnFe_2O_4$ nanoparticles are nearly 1.64, 1.62, 1.59, 1.53 and 1.47eV. **Fig. 6** showed that the band gap energy values decreased with increase in temperature.

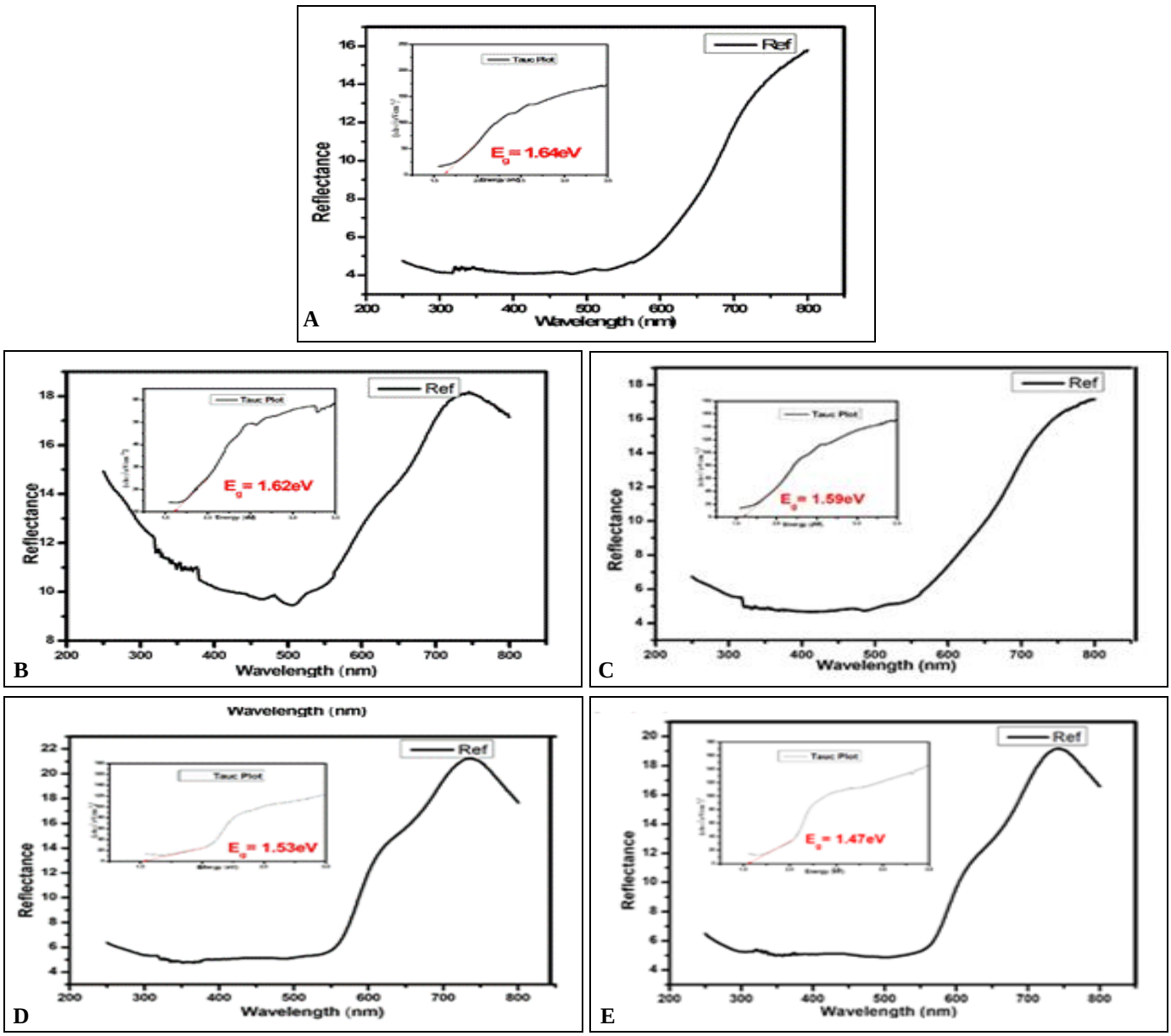

FIG. 6: TAUC PLOT OF hυ *vs.* (αhυ)2 FOR ZINCFERRITE NANOPARTICLES WAS ANNEALED AT (A) 400, (B) 500, (C) 600, (D) 700, AND (E) 800 ºC

Antioxidant Activity: The antioxidant activity of $ZnFe_2O_4$ nano-particles were determined by using DPPH radical scavenging assay method. In the present study the antioxidant activity at different annealing temperatures were noted. In each temperature, the variation of inhibition corresponding to different concentration was analyzed and depicted in **Fig. 7**. From the graph it was observed that with each annealing temperature, as the concentration of synthesized $ZnFe_2O_4$ nanoparticles increased, the anti-oxidant activity also increased and it was also observed that at different calcination temperature 500, 600, 700, 800 ºC for 4 h. The lower concentration such as (12.5 mg/mL, 25 mg/mL, 50 mg/mL) with their inhibition rate was more than that of the standard (Ascorbic Acid).The higher concentrations such as (100 mg/mL & 200 mg/mL), the inhibition rate was gradually decreasing as compared with the standard, but at higher annealing temperature 800 ºC for 4 h. the antioxidant activity was suddenly decreased. The antioxidant activity could be

associated with the transfer of free electrons from the oxygen atom of nanoparticles to free radicals present in the nitrogen atom of DPPH molecules. The antioxidant activity was mainly attributed to high surface to volume ratio of nano architecture.

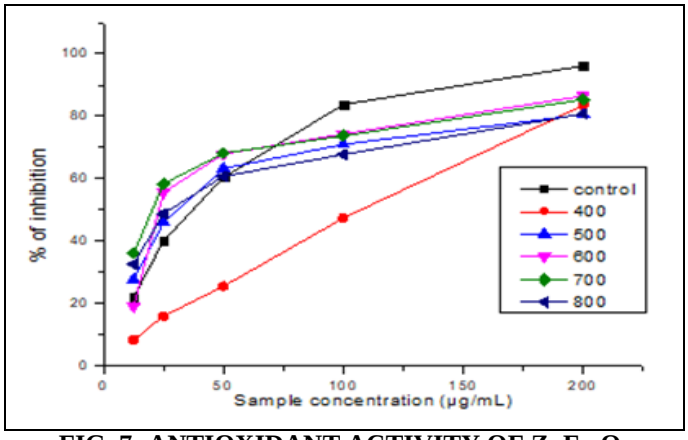

FIG. 7: ANTIOXIDANT ACTIVITY OF $ZnFe_2O_4$ NANOPARTICLES AT DIFFERENT TEMPERATURES

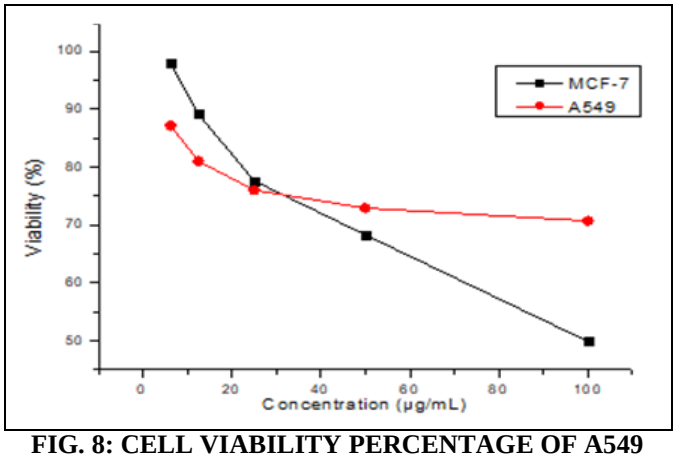

FIG. 8: CELL VIABILITY PERCENTAGE OF A549 (LUNG- CANCER CELL) AND MCF – 7 *vs.* $ZnFe_2O_4$

Analysis of Cytotoxicity: The cytotoxic activity of $ZnFe_2O_4$ nanoparticles at different concentration against the MCF - Cells (Human breast adenocarcinoma Cell line) and A549 (Lung-Cancer Cell) using MTT assay shown in **Fig. 8**.

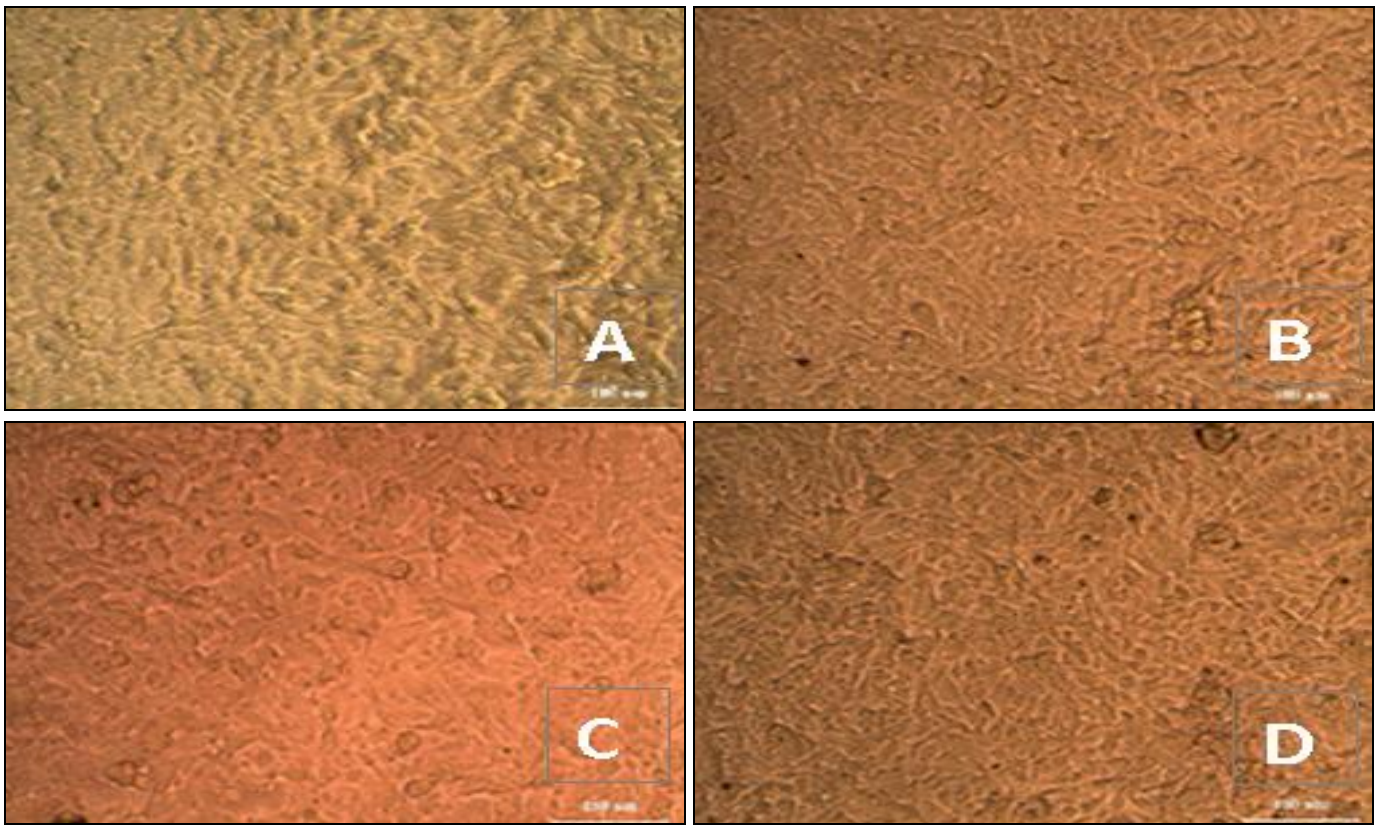

FIG.9: (A) UNTREATED LUNG CANCER CELL LINE, (B) SAMPLE CONCENTRATION OF 25 µg/mL $ZnFe_2O_4$ (C) 50 µg/mL $ZnFe_2O_4$, (D) 100 µg/mL $ZnFe_2O_4$

The test outcome revealed that in the case of zinc ferrite nanoparticles against A549 (Lung cancer) Cell, the cancer cell death increases as the concentration of $ZnFe_2O_4$ increases. The addition of 6.25 µg/mL of $ZnFe_2O_4$ showed the cell viability of 87.12%. 12.5 µg/mL with 81.04% of cell viability, 25 µg/mL with 76% of cell viability, 50 µg/mL with 72.9% of cell viability and 100 µg/mL

with 70.67% of cell viability. In MCF – 7 (Human breast adenocarcinoma) cell line investigated that the amount of $ZnFe_2O_4$, nanoparticles as well as the cancer cell death increased. The addition of 6.5 µg/mL of $ZnFe_2O_4$ showed a the cell viability of 97.28%, 12.5 µg/mL with 89.18% cell viability, 25 µg/mL with 77.61% cell viability, 50 µg/mL with 68.26% cell viability and 100 µg/mL with 49.84% cell viability. From this study it was confirmed that as the concentration of zincferrite nanoparticles increases, the breast cancer cell death increases. The highest cell viability (100%) observed at 0 µg/mL started to decrease gradually with the increased concentration.

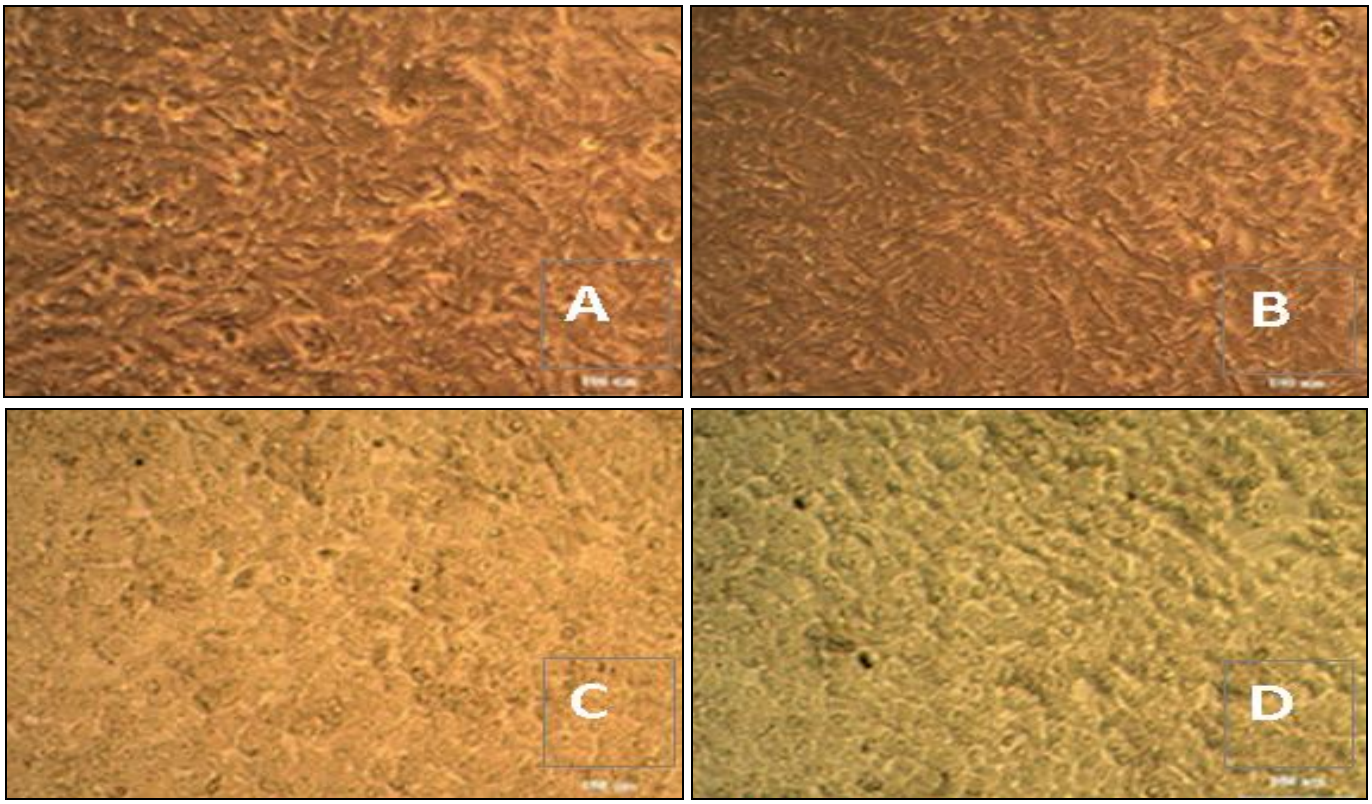

FIG. 10: (A) UNTREATED BREAST CANCER CELL LINE, (B) SAMPLE CONCENTRATION OF 6.25 µg/ml $ZnFe_2O_4$, (C) 50 µg/ml $ZnFe_2O_4$, AND (D) 100 µG/ML $ZnFe_2O_4$

The **Fig. 8** clearly pointed out that $ZnFe_2O_4$ 500 ºC, 4 h. nanoparticles possessed less viability towards MCF – 7 cells (Human breast adenocarcinoma) than A 549 (lung cancer cell) at higher concentrations. It was also observed that the cell survival capacity decreased promptly in MCF – 7 cell with the increase in concentrations of $ZnFe_2O_4$ nanoparticles whereas the viability was moderately decreased in A 549 (lung cancer cell) with increase in the concentration of $ZnFe_2O_4$ nanoparticles.

Antibacterial and Antifungal Activity: The antibacterial activity of $ZnFe_2O_4$ nanoparticles was studied against gram negative *E. coli* bacterial strain using agar well diffusion method. Significant antibacterial activity was observed against *E. coli* and displayed nearly uniform inhibition rate (10-12) at different annealing temperature in high concentrations such as 500 µg/mL and 100 µg/mL. The zone of inhibition was represented in mm **Fig. 12**. The effect of $ZnFe_2O_4$ nanoparticles on bacterial linear growth revealed that the bacterial growth was reduced by increasing the concentration as well as higher calcinations temperatures **Fig. 11A**.

The antifungal study demonstrated that the percentage of inhibition was found to be increased up to certain annealing temperature (600 °C), further rise in temperature the antifungal activity of synthesized $ZnFe_2O_4$ nanoparticle was decreased and the rate of inhibition was found to be suddenly reduced. The variation of inhibition rate against different annealing temperature is graphically displayed in **Fig. 11B**.

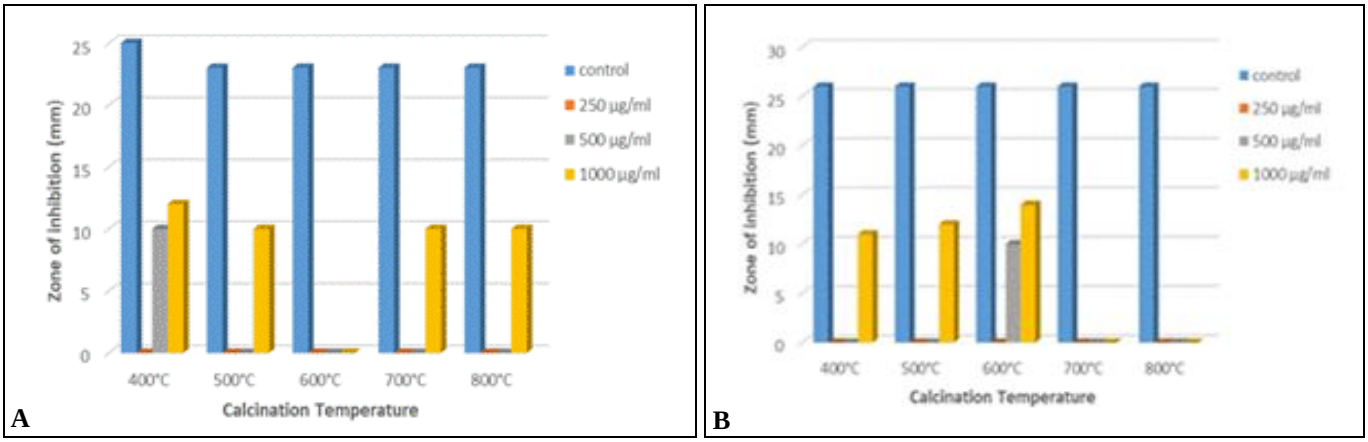

FIG. 11: PERCENTAGE OF INHIBITION OF SAMPLE AT DIFFERENT CONCENTRATION. 250 µg/ml, 500 µg/ml, 1000 µg/ml AT DIFFERENT ANNEALING TEMPERATURE AGAINST (A) *E. COLI* (ATCC 25922), GRAM NEGATIVE (B). *ASPERGILLUS NIGER* (ATCC 16404)

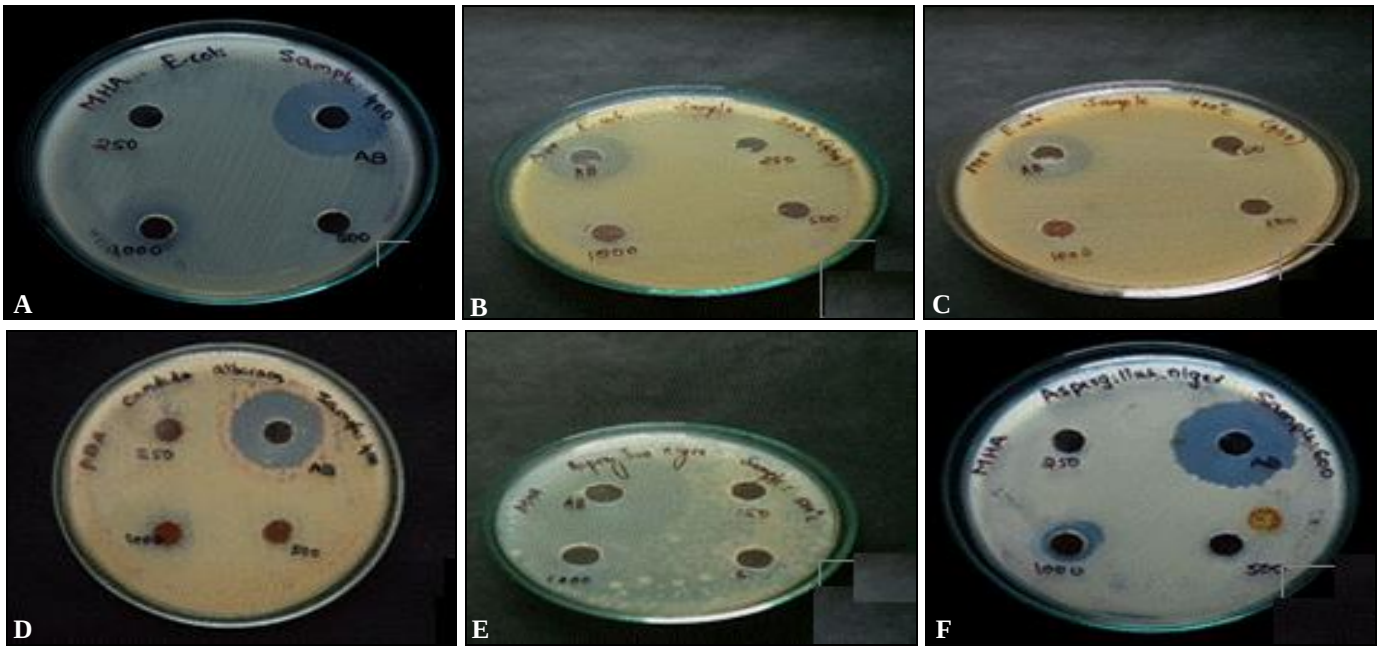

FIG. 12: ANTIBACTERIAL ACTIVITY AND ANTIFUNGAL ACTIVITY OF $ZnFe_2O_4$ NANOPARTICLES. FIG (A, B, C) *E. COLI* GRAM NEGATIVE- ZONE OF INHIBITION 12 MM, 10 MM, 10 MM AND FIG (D, E, F) *ASPERGILLUS NIGER* – ZONE OF INHIBITION 11, 12 AND 14 MM

CONCLUSION: $ZnFe_2O_4$ nanoparticles were simply and successfully prepared by a low cost co precipitation method using PEG as the Capping agent. Structural characteristics and biological properties of prepared samples were well studied. The XRD result confirmed the crystallite size and X-ray density was identified to be increased with increase in annealing temperature whereas lattice constant tent to be decreasing. The crystallite size calculated from XRD data using Debye Scherer method well matches with the calculated particle size from FESEM. Morphological study of FESEM showed that the synthesized $ZnFe_2O_4$ particles posessed spherical morphology. Presence of zinc ferrite nano-particles at different annealing temperatures were confirmed from FTIR results and a decrease in band gap energy with increase in temperature was obtained using UV-Visible result analysis.

The results of *in-vitro* cytotoxic, anti-bacterial, anti-fungal and antioxidant activity showed that the synthesized $ZnFe_2O_4$ nanoparticles can be used for bio medical applications. The $ZnFe_2O_4$ nano-particles were more reactive towards MCF-7 (Human breast adenocarcinoma) and DPPH free radical scavenging activity. The results revealed that the particle size and annealing temperature strongly influenced the described behaviour.

ACKNOWLEDGEMENT: We are deeply acknowledged to the principal, Mar Ivanios College, Thiruvananthapuram, Kerala for providing necessary facilities for doing this work.

CONFLICTS OF INTEREST: We declare that no conflicts of interest.

REFERENCES:

1. Sivagurunathan P and Sathiyamurthy K: Effect of temperature on structural, morphological and magnetic properties of zinc ferrite nanoparticles. Canadian Chemical Transaction 2016; 4: 244-54.
2. Ebrahimi M, Shahraki RR, Ebrahimi SAS and Masoudpanah SM: Magnetic properties of zinc ferrite nanoparticles synthesized by coprecipitation method. J Supercond Nov Magn 2014; 27: 1587-92.
3. Deraz NM and Shaban S: Optimization of catalytic, surface and magnetic properties of nanocrystalline manganese ferrite. J Analyt Appl Pyrolysis 2009; 86(1): 173-79.
4. Kamari N, Kumar V, Khasa S and Singh SK: Structural and dielectric investigations of ferrite nanoparticles prepared by chemical co-precipitation method. Journal of Advanced Physics 2014; 3: 1-5.
5. Maria M, Sinthiya A, Ramamurthi K, Madhuri S, Manimozhi T, Kumareshan N, Margoni MM and Karthika PC: Synthesis of zinc ferrite nanoparticles with different capping agent. International Journal of Chem Tech 2015; 7: 2144-49.
6. Kulkarni AB and Mathad SN: Variation in structural and mechanical properties of CD-doped Co-Zn ferrites. Materials Science for Energy Technologies 2019; 2: 455-62.
7. Okoroh DO and Asogwa PU: Thermal treated synthesis and characterization of polyethylene glycol (PEG) mediated zinc ferrite nanoparticles. Surfaces and Interfaces 2019; 16: 127-31.
8. Petova E and Fahmi A: Influence of synthesis methods on structural and magnetic characteristics of mg-zn ferrite nano powders. Journal of Magnetism and Magnetic Materials 2019: 473: 85-91.
9. Sivagurunathan P and Sathiyamurthy K: Effect of temperature on structural, morphological and magnetic properties of zinc ferrite nanoparticles. Canadian Chemical Transaction 2016; 4: 244-54.
10. Anilkumar MR, Nagaswarupa HP, Nagabhushana H, Sharma SC, Vidya YS, Anantharaju KS, Prashantha SC, Shivakuamra C and Gurushantha K: Bio-inspired route for the synthesis of spherical shaped MgO:Fe^{3+} nanoparticles structural, photoluminescence and photo catalytic investigation. Molecular and Biomolecular Spectroscopy 2015; 149: 703-13.
11. Anooj ES, Sreelekshmi SJ, Gopukumar ST and Praseetha PK: Evaluation of the zinc ferrite nanoparticles for Bio-applications. IJPSR 2017; 04: 22-26.
12. Jermy BR, Ravinayagam V, Widyan A, Alamoudi, Almohazey D, Dafalla H, Allehaibi LH, Baykal A, Muhammet S, Toprak and Somanathan T: Targeted therapeutic effect against the brest cancer cell line MCF-7 with a $CuFe_2O_4$ / Silica / Cisplatin Nanocomposit Formulation. Journal of Nanotechnology 2019; 10: 2217-28.
13. Vijayakumar S and Vaseeharan B: Anticancer and ecotoxicity properties of collagen based ZnO nano-particles. Adv Power Techno 2018; 29(10): 2331-45.
14. Rajiv P and Jacob V: *In-vitro* analysis- the anti-microbial and anti-oxidant activity of zinc oxide nanoparticles from *Curcuma longa*. Asian Journal of Pharmaceutical and Clinical Research 2019; 12: 200-4.
15. Manyasree D, Kiranmayi P and Kolli VR: Nanaometal oxides as Anti-microbial Agents (Al_2O_3, CuO, Fe_3O_4 and ZnO) Comparative study. Indo American Journal of Pharmaceutical Research 2019; 2231-76
16. Rehm S, Ansari MA, Alzohairy MA, Alomary MN, Jermy BR, Shahzad R, Tashkandi N and Alsalem ZH: Anti-bacterial and Antifungal activity of novel synthesized Neodymium-Substituted Cobalt ferrite nanoparticles for biomedical application. MDPI 2019; 7(10): 714.
17. Ravi C, Bharamagouder, Patil AS, Mathad SN, Kumbar VM, Laxmi B and Kankanawadi: Magnetic and Anti-Bacterial studies of nano-ferrites Prepared by Self propagating high-temperature synthesis route. Sciendo 2018; 26(2): 249-62.
18. Sinthiya MMA, Ramamurthi K, Mathuri S, Manimozhi T and Kumaresan N: Synthesis of Zinc Ferrite ($ZnFe_2O_4$) Nanoparticles with Different capping agents. Int J Chem Tech 2015; 7: 2144-49.
19. Sharma N, Aghamkar P, Kumar S, Bansal M, Anju and Tondon RP: Study of structural and magnetic properties of ND dopped zinc ferrites. Journal of Magnetism and Magnetic Materials 2014; 369: 162-67.
20. Kumar RR and Venimadhav A: Weak ferromagnetism in band-gap engineered α-(Fe2O3)1-X(Cr_2O_3)X Nano-particles. IEEE 2019; 473: 119-24.

How to cite this article:
Jyothish B and Jacob J: Effect of temperatures on structural, morphological and bio-properties of zinc ferrite nanoparticles. Int J Pharm Sci & Res 2020; 11(12): 6391-01. doi: 10.13040/IJPSR.0975-8232.11(12).6391-01.